

AKLT Models with Quantum Spin Glass Ground States

C. R. Laumann, S. A. Parameswaran, and S. L. Sondhi
*Department of Physics, Joseph Henry Laboratories,
Princeton University, Princeton NJ 08544, USA*

F. Zamponi
*Laboratoire de Physique Théorique, Ecole Normale Supérieure,
UMR CNRS 8549, 24 Rue Lhomond, 75231 Paris Cedex 05, France*
(Dated: February 23, 2024)

We study AKLT models on locally tree-like lattices of fixed connectivity and find that they exhibit a variety of ground states depending upon the spin, coordination and global (graph) topology. We find a) quantum paramagnetic or valence bond solid ground states, b) critical and ordered Néel states on bipartite infinite Cayley trees and c) critical and ordered quantum vector spin glass states on random graphs of fixed connectivity. We argue, in consonance with a previous analysis¹, that *all* phases are characterized by gaps to local excitations. The spin glass states we report arise from random long ranged loops which frustrate Néel ordering despite the lack of randomness in the coupling strengths.

I. INTRODUCTION

The study of quantum antiferromagnets has proven among the most enduring themes in modern condensed matter physics. The interplay between frustration and quantum fluctuations leads such systems to exhibit a variety of interesting ground states. In this context the lattice models constructed by Affleck *et al.*^{2,3} are particularly useful for they build in a great deal of both these effects using simple local projectors, which allow their ground states to be determined analytically. These AKLT models have spins given by $S = \frac{z}{2}M$, where M is a positive integer, and z the lattice coordination number. In principle, they may be defined on any graph, but in practice one usually maintains fixed connectivity in order to have the same spin on each site. The associated ground states have the added feature that their wavefunctions can be written in Jastrow (pair product) form, which allows us to view their ground-state probability densities as Boltzmann weights corresponding to a nearest neighbor Hamiltonian for classical vector spins on the *same* lattice. Using this unusual quantum-classical equivalence one can understand many properties of the states by studying the associated classical model.

The initial construction of the AKLT models was motivated by the search for quantum disordered states in low dimensions. This works only too well: in $d = 1$ and $d = 2$ the mapping to finite temperature classical models discussed above ensures, by the Mermin-Wagner theorem, that *all* cases lead to quantum paramagnetic or valence bond solid ground states. In $d > 2$ this is no longer true and a computation is needed to decide which models order and which do not. In a recent paper, Parameswaran, Sondhi and Arovas⁴ showed via Monte Carlo simulations and mean-field arguments that AKLT models on the diamond and pyrochlore lattices exhibit quantum-disordered ground states for small spin sizes while on the cubic lattice all models exhibit Néel order.

In this paper we take this exploration of higher dimen-

sional AKLT models in a different direction—we study them on locally tree-like lattices of fixed connectivity z , which are known to physicists as Bethe lattices. Here we shall consider two physically distinct systems. The first, is the Bethe lattice constructed as the limit of a family of Cayley trees. This construction yields a system with a finite surface to volume ratio and without loops. The second is a typical member of the ensemble of random graphs of fixed connectivity. These graphs are locally tree-like in the thermodynamic limit; however they also have long loops of logarithmically divergent size. These loops of both even and odd lengths introduce topological frustration into the system. The two constructions of locally tree-like lattices yield different physics.

For the infinite Cayley tree, we exhibit an exact solution using the quantum-classical correspondence. Specifically, we use a generalized transfer matrix technique to obtain exact solutions for various statistical quantities in the ground state of the tree. We note that the AKLT model on the Bethe lattice has been studied before directly within the quantum formalism⁵; we suspect that readers will find our solution simpler. We find one quantum disordered state ($M = 1$ on the $z = 3$ tree) and two that are critical ($M = 2$ on $z = 3$ and $M = 1$ on $z = 4$), in that the correlation functions decay exponentially at precisely the rate required to balance the exponential growth of the graph. All other cases exhibit Néel order. We address the question of whether the bulk excitations are gapless in cases when the AKLT wavefunction has critical or Néel correlations. We find, perhaps surprisingly, that the system is always gapped to *local* excitations, and that the only gapless excitation is a global one connecting the different broken-symmetry ground states. We connect this to related work in Ref. 1, in which we conjecture that this is a generic feature of symmetry breaking quantum models on the Bethe lattice, related to the spectrum of the graph Laplacian.

On random graphs of fixed connectivity, Néel ordering in the companion classical model is frustrated by the

presence of the long loops. To study this case, we appeal to the cavity techniques familiar from the theory of classical disordered systems. These have been applied recently to a variety of discrete statistical mechanical problems on random graphs and there is much evidence that the (approximate) techniques are on solid ground. From this analysis, we conclude that for $z \leq 10$ there are disordered states at small spin and spin glass ground states at larger spin as well as a couple of cases where the state is critical. For $z > 10$ all AKLT models have ground states with spin glass order. By spin glass order, we mean states with fixed but randomly oriented local magnetizations and that the set of such states is larger than those connected by global rotations alone. We argue that the spectrum of local excitations above the pure states in this set is again gapped.

Of our various results we would especially like to flag these last mentioned. The nature of quantum glass phases is a subject of much interest – especially as to how much of the elaborate framework of the classical subject may be lifted into the quantum world. The AKLT construction provides a direct line of approach to this problem and does so using Hamiltonians without random couplings but from graph disorder alone.

This paper is organized as follows: in Section II, we introduce the AKLT model on an arbitrary graph via the Schwinger boson formalism. We proceed to construct a companion classical model that captures the structure of the ground state wavefunction by introducing a basis of $SU(2)$ coherent states. In Section III, we develop transfer-matrix technology to solve the companion classical model on the (bipartite) Bethe lattice exactly, and obtain the transition temperature and correlation functions in the paramagnetic and Néel-ordered phases. In Section IV we investigate the energy gap using a variational *ansatz* for the excited states. Finally, in Section V we consider the extension of this analysis to the spin glass transition expected on regular random graphs and consider some of the quantum consequences of the classical glassy phase.

II. AKLT STATES: A BRIEF REVIEW

The central idea of the AKLT approach³ is to use quantum singlets to construct correlated quantum-disordered wavefunctions, which are eigenstates of local projection operators. One can then produce many-body Hamiltonians using projectors that extinguish the state, thereby rendering the parent wavefunction an exact ground state, often with a gap to low-lying excitations. A general member of the family of valence bond solid (AKLT) states can be written compactly in terms of Schwinger bosons⁶:

$$|\Psi(M)\rangle = \prod_{\langle ij \rangle} \left(b_{i\uparrow}^\dagger b_{j\downarrow}^\dagger - b_{i\downarrow}^\dagger b_{j\uparrow}^\dagger \right)^M |0\rangle. \quad (1)$$

This assigns M singlet creation operators to each link $\langle ij \rangle$ of an underlying lattice. The total boson occupancy

per site is given by zM , where z is the lattice coordination number, and the resultant spin on each site is given by $S = \frac{1}{2}zM$. Given any regular graph, the above construction defines a family of AKLT states labeled by the size of their spins $S = \frac{1}{2}zM$. For more details regarding this construction and the corresponding Hamiltonians, see Ref. 4.

The AKLT states have a convenient representation in terms of $SU(2)$ coherent states, as first shown in Ref. 6. In terms of the Schwinger bosons, the normalized spin- S coherent state is given by $|\hat{n}\rangle = (p!)^{-1/2} (z_\mu b_\mu^\dagger)^p |0\rangle$, where $p = 2S$, with $z = (u, v)$ a \mathbb{CP}^1 spinor, with $u = \cos(\theta/2)$ and $v = \sin(\theta/2)e^{i\varphi}$. The unit vector \hat{n} is given by $n^a = z^\dagger \sigma^a z$, where σ are the Pauli matrices. In the coherent state representation, the general AKLT state wavefunction is the pair product $\Psi(\{\hat{n}_i\}) = \langle \{\hat{n}_i\} | \Psi \rangle = \prod_{\langle ij \rangle} (u_i v_j - v_i u_j)^M$. Following Ref. 6, we may write $|\Psi(\{\hat{n}_i\})|^2 \equiv \exp(-\beta H_{\text{cl}})$ as the Boltzmann weight for a classical $O(3)$ model with Hamiltonian

$$H_{\text{cl}} = - \sum_{\langle ij \rangle} \ln \left(\frac{1 - \hat{n}_i \cdot \hat{n}_j}{2} \right), \quad (2)$$

at inverse temperature $\beta = M$. All equal time quantum correlations in the state $|\Psi\rangle$ may then be expressed as classical, finite temperature correlations of the Hamiltonian H_{cl} .

Some immediate consequences of this quantum-to-classical equivalence were noted in Ref. 6. On one and two-dimensional lattices, the Hohenberg-Mermin-Wagner theorem precludes long-ranged order at any finite value of the discrete quantum parameter M . In three dimensions, there is no *a priori* reason to rule out long-range order. In fact, as shown in Ref. 4, the simple cubic lattice has no quantum-disordered states at any M , while the diamond lattice has a single such state for $M = 1$; on frustrated lattices such as the pyrochlore, such states are believed to exist for many values of M .

As is evident from (1), we may define the AKLT states on an arbitrary graph; if the graph has fixed connectivity z , then the resulting model has the same spin on each site. On graphs with a boundary, this is not automatic, since the boundary sites will have fewer neighbors z' . There are several ways to deal with this boundary effect. The first is to work with a system with a lower spin on the boundary: in that case $S' = \frac{1}{2}z'M$. The quantum state of this non-homogeneous system is unique. Another option is to add $(z - z')$ additional Schwinger bosons of either flavor to the edge sites; there is not a unique way in which to do this, leading to a multitude of degenerate ground states classified by the state of the boundary spins. When translated to the companion classical model, the latter option can be viewed as connecting each of the boundary spins to $(z - z')$ fixed spins, each with an orientation specified by the behavior of an independent spin-1/2 degree of freedom; thus, the different degenerate states of the homogeneous AKLT model on a graph with boundary can be understood by choosing different fixed boundary

conditions for spins in an additional, outer ring of leaf spins. Finally, one can opt to get rid of the boundary by, for instance, taking periodic boundary conditions on a Euclidean lattice. As we will discuss in Sec. V, when generalized to tree-like graphs, this approach leads to a spin glass phase in the companion model and thus provides a non-trivial new quantum spin glass to the AKLT phase diagram.

III. TRANSFER MATRIX SOLUTION OF THE CLASSICAL PROBLEM ON TREES

The classical Hamiltonian that describes the properties of the ground-state wavefunction of an AKLT model with singlet index M , written in the basis of $SU(2)$ coherent states is given by

$$\beta H_{\text{cl}} = -M \sum_{\langle i,j \rangle} \log \left[\frac{1 - \hat{n}_i \cdot \hat{n}_j}{2} \right] \quad (3)$$

Before we proceed, we note that on bipartite graphs we can perform a gauge transformation by flipping every spin at odd depth to obtain a ferromagnetic model. This gives us

$$\beta H_{\text{cl}} = -M \sum_{\langle i,j \rangle} \log \left[\frac{1 + \hat{n}_i \cdot \hat{n}_j}{2} \right] \quad (4)$$

As usual in the treatment of tree models, we consider the statistical state $\psi^0(\hat{n}_0)$ (marginal distribution) of a cavity spin \hat{n}_0 at the root of a branch of the tree. This unnormalized distribution can be found in terms of the cavity states of its $z-1$ neighbors by summation:

$$\begin{aligned} \psi^0(\hat{n}_0) &= \int D\hat{n}_1 \cdots D\hat{n}_{z-1} T(\hat{n}_0, \hat{n}_1) \psi^1(\hat{n}_1) \cdots T(\hat{n}_0, \hat{n}_{z-1}) \psi^{z-1}(\hat{n}_{z-1}) \\ &= \int D\hat{n}'_1 \cdots \hat{n}'_{z-1} M(\hat{n}_0; \hat{n}'_1, \dots, \hat{n}'_{z-1}) \int D\hat{n}_1 \cdots D\hat{n}_{z-1} T(\hat{n}'_1, \hat{n}_1) \psi^1(\hat{n}_1) \cdots T(\hat{n}'_{z-1}, \hat{n}_{z-1}) \psi^{z-1}(\hat{n}_{z-1}) \end{aligned} \quad (5)$$

where

$$T(\hat{n}_0, \hat{n}_1) = e^{\beta \log \left[\frac{1 + \hat{n}_0 \cdot \hat{n}_1}{2} \right]} = \left(\frac{1 + \hat{n}_0 \cdot \hat{n}_1}{2} \right)^\beta \quad (6)$$

is the transfer matrix of the AKLT model and

$$M(\hat{n}_0; \hat{n}'_1, \dots, \hat{n}'_{z-1}) = \delta(\hat{n}_0 - \hat{n}'_1) \cdots \delta(\hat{n}_0 - \hat{n}'_{z-1}) \quad (7)$$

is the merge matrix.

The merge matrix M defines a multilinear map from the $z-1$ state spaces of the neighbor spins to the state space of the root. This lifts naturally to the appropriate complexified tensor product spaces²⁷ and thus we will find it natural to write the merge and transfer operations abstractly using Dirac notation:

$$\begin{aligned} M &= \int D\hat{n}_0 D\hat{n}'_1 \cdots D\hat{n}'_{z-1} \delta(\hat{n}_0 - \hat{n}'_1) \cdots \delta(\hat{n}_0 - \hat{n}'_{z-1}) |\hat{n}_0\rangle \langle \hat{n}'_1| \cdots \langle \hat{n}'_{z-1}| \\ &= \int D\hat{n} |\hat{n}\rangle \langle \hat{n}| \cdots \langle \hat{n}| \end{aligned} \quad (8)$$

and,

$$T = \int D\hat{n} D\hat{n}' T(\hat{n}, \hat{n}') |\hat{n}\rangle \langle \hat{n}'|. \quad (9)$$

Thus, equation (5) becomes

$$|\psi^0\rangle = M (T|\psi^1\rangle \otimes \cdots \otimes T|\psi^{z-1}\rangle). \quad (10)$$

We now focus on the stability of the paramagnetic state against Néel ordering. Hence, we have to use boundary

conditions that are consistent with this kind of ordering. As discussed at the end of Section II, one can either use free boundary spins with lower S , or connect the boundary spins to some fixed additional spins: in the latter case, the additional spins must all have the same orientation to allow the Néel ordering. This remark is particularly important because, as we will see later in Section V, on a random regular graph the boundary conditions on any given tree-like subregion are fixed self-consistently,

and in general are not consistent with Néel ordering, leading to a disordered spin glass state. Assuming uniform boundary conditions, we obtain the unique state at depth $d - 1$ by merging the $z - 1$ states at level d using the T and M operators:

$$|d - 1\rangle = M(T|d\rangle)^{\otimes(z-1)}. \quad (11)$$

The natural basis to work in is that of states with definite angular momentum, i.e. states $|lm\rangle$, which are

$$\begin{aligned} M &= \int D\hat{n} |\hat{n}\rangle\langle\hat{n}| \cdots \langle\hat{n}| \\ &= \int D\hat{n} \sum_{l_0, m_0} \sum_{l_1, m_1} \cdots \sum_{l_{z-1}, m_{z-1}} |l_0, m_0\rangle\langle l_0, m_0| \hat{n} (\langle\hat{n}|l_1, m_1\rangle\langle l_1, m_1| \otimes \cdots \otimes \langle\hat{n}|l_{z-1}, m_{z-1}\rangle\langle l_{z-1}, m_{z-1}|) \\ &= \sum_{l_0, m_0} \sum_{l_1, m_1} \cdots \sum_{l_{z-1}, m_{z-1}} |l_0, m_0\rangle (\langle l_1, m_1| \otimes \cdots \otimes \langle l_{z-1}, m_{z-1}|) \int D\hat{n} Y_{l_0}^{m_0*}(\hat{n}) Y_{l_1}^{m_1}(\hat{n}) \cdots Y_{l_{z-1}}^{m_{z-1}}(\hat{n}) \end{aligned} \quad (12)$$

For the case $z = 3$, the integral in (12) is simply the Clebsch-Gordan coefficient that characterizes the fusion of two $SU(2)$ spins. For higher values of z , this is the appropriate generalization of the Clebsch-Gordan coefficient describing the fusion of $(z - 1)$ $SU(2)$ spins. Thus we see that the merge operation, when written in the angular momentum basis, has a natural interpretation as the fusion rules for the $O(3)$ symmetry group.

The paramagnetic state - here represented in Fourier space by the $|00\rangle$ state - is always a fixed point: it is an eigenstate of the T -matrix, and the fusion of any number of $|00\rangle$ states is again a $|00\rangle$ state. We proceed via linear stability analysis: we introduce a perturbation into a state that is not uniformly weighted on the sphere, and see if this grows or shrinks under the iteration procedure. We note that we can decompose any such state into spherical harmonics, and so we write $|d\rangle = |00\rangle + \epsilon \sum_{l \neq 0, m} c_{lm} |lm\rangle$ into (11) to obtain

$$\begin{aligned} |d - 1\rangle &= M \left(\lambda_0 |00\rangle + \epsilon \sum_{l \neq 0, m} \lambda_l c_{lm} |lm\rangle \right)^{\otimes(z-1)} \\ &= \lambda_0^{z-1} |00\rangle \\ &\quad + \epsilon(z-1) \lambda_0^{z-2} \sum_{l \neq 0, m} \lambda_l c_{lm} |lm\rangle + \mathcal{O}(\epsilon^2) \end{aligned} \quad (13)$$

where we have used the fact that fusing any number of $|00\rangle$ states with an $|lm\rangle$ state results in an $|lm\rangle$ state. We renormalize to leading order and find that the iterated state is, to linear order

$$|d - 1\rangle = |00\rangle + \epsilon(z-1) \sum_{l \neq 0, m} \frac{\lambda_l}{\lambda_0} c_{lm} |lm\rangle + \mathcal{O}(\epsilon^2) \quad (14)$$

eigenstates of the angular momentum operators L^2, L_z . In the coordinate basis, these are simply the spherical harmonics, and as shown in Appendix A, they are eigenstates of the transfer matrix with eigenvalue λ_l .

It remains for us to understand exactly how the merge operation acts in the angular momentum basis. If we insert resolutions of the identity in the angular momentum basis into (8), we obtain

The perturbation is irrelevant (shrinks under iteration) if the coefficient of the linear term is less than 1, and relevant if it is greater than 1. The critical point is reached when

$$\frac{\lambda_l}{\lambda_0} = \frac{1}{z-1} \quad (15)$$

for any l . Using the temperature dependent expression (A4) for the λ_l , one can show that the dipole instability ($l = 1$) is the first one encountered as the temperature is lowered, and therefore sets the transition temperature.

Using the results of Appendix A (replacing β by the singlet parameter M), we obtain

$$M_c = \frac{2}{z-2} \quad (16)$$

We see that for $z = 2, 3, 4$, $M_c = \infty, 2, 1$, while for all other values, $M_c < 1$. Since M must be a positive integer, we see that for the chain ($z = 2$) all values of M correspond to quantum-disordered states (which follows from the Mermin-Wagner theorem and the original AKLT result²) whereas for $z = 3$, the $M = 1$ state is disordered while the $M = 2$ state is critical, and finally for $z = 4$, the $M = 1$ state is critical. Bethe lattices of higher connectivity will always have ordered AKLT ground states for any value of M . See Fig. 1.

Finally, we consider the correlation function $\langle \hat{n}_0 \cdot \hat{n}_d \rangle$ within the paramagnetic phase. This is given by considering the response of $\langle \hat{n}_0 \rangle$ to a field on \hat{n}_d - which is the same as asking how the dipole $l = 1$ perturbation propagates along a chain of length d in a background of trivial $l = 0$ cavity states. This immediately implies

$$\langle \hat{n}_0 \cdot \hat{n}_d \rangle \propto \left(\frac{\lambda_1}{\lambda_0} \right)^d = \left(\frac{M}{M+2} \right)^d \quad (17)$$

Notice that this implies that the naive correlation length never diverges – as usual with tree models, phase transitions occur when the correlation decays at the same rate as the growth of the lattice. For a slightly more detailed calculation, see Appendix B.

As an aside, we note that we can use the same generalized transfer matrix technique to obtain the transition temperature for the Heisenberg model, a result first obtained by Fisher⁷ using a different method. This serves as a test of the technique proposed here.

IV. VARIATIONAL BOUNDS ON THE GAP

We now perform a variational computation of the gap to excitations in the critical model, similar to the Single-Mode Approximation (SMA) discussed in Ref. 6. The central idea of the SMA is to construct an excitation orthogonal to the ground state by acting on it with a local operator, and then to reduce the energy of this excitation by delocalizing it, thereby decreasing its kinetic energy. A variational bound on the energy gap is given by

$$0 \leq \Delta \leq \Delta_{SMA} = \frac{\langle \Psi_{SMA} | H - E_0 | \Psi_{SMA} \rangle}{\langle \Psi_{SMA} | \Psi_{SMA} \rangle} \quad (18)$$

This approach is designed to optimize the energy due to the off-diagonal matrix elements in the excited sector, which will be proportional to the usual graph Laplacian for a nearest neighbor model. On the Bethe lattice, the spectrum of the Laplacian is unusual. As argued in Ref. 1, there is necessarily a gap to hopping excitations on tree-like graphs despite the existence of symmetry related ground states. Thus, in some sense the SMA calculation is doomed to failure as it will never be able to close this gap. Nonetheless, it is interesting to see how this plays out in an exact model.

We consider a rooted Cayley tree, and in order to restrict ourselves to studying excitations confined to the bulk as the size of the tree grows we suppress excitations far from the center using an infrared regulator λ . We therefore study variational wavefunctions of the form

$$|\Psi_{SMA}\rangle = |\lambda\rangle = \sum_{i=1}^N u_\lambda(i) S_i^z |\Psi\rangle \quad (19)$$

where $u_\lambda(i)$ is a function only of the depth ρ_i of site i referenced to the root of the Cayley tree. The SMA gap is

$$\Delta_{SMA} = \lim_{\lambda \rightarrow 0} \left[\lim_{N \rightarrow \infty} \frac{\langle \lambda | H - E_0 | \lambda \rangle}{\langle \lambda | \lambda \rangle} \right] \quad (20)$$

After some algebra, we may write (with the understanding that we always take N to infinity *before* taking λ to zero):

$$\Delta_{SMA} = \lim_{\substack{N \rightarrow \infty \\ \lambda \rightarrow 0}} \left[\frac{\sum_{i,j} u_\lambda(i) u_\lambda(j) \langle [S_i^z, [H, S_j^z]] \rangle_\Psi}{\sum_{i,j} u_\lambda(i) u_\lambda(j) \langle S_i^z S_j^z \rangle_\Psi} \right] \quad (21)$$

Asserting homogeneity of the graph, and noting that the Hamiltonian is a function only of $S_i \cdot S_j$ where i and j are nearest neighbors, we may re-express this as

$$\Delta_{SMA} = \lim_{\substack{N \rightarrow \infty \\ \lambda \rightarrow 0}} \left[f \times \frac{\sum_{i,j} u_\lambda(i) \mathcal{A}_{ij} u_\lambda(j)}{\sum_{i,j} u_\lambda(i) \gamma^{|i-j|} u_\lambda(j)} \right] \quad (22)$$

where $f = \frac{1}{4} \langle [S_i^z - S_j^z, [H, S_i^z - S_j^z]] \rangle_\Psi$, and we denote by \mathcal{A} the adjacency matrix of the Cayley tree; the correlations in the ground state are always exponential, and go as $\gamma^{|i-j|}$, where $\gamma \rightarrow \frac{1}{z-1}$ from below as we approach criticality. We have therefore reduced the problem of the SMA on the Bethe lattice to understanding (i) the spectrum of the graph Laplacian (the adjacency matrix up to a sign) and (ii) the behavior of the ground-state correlations.

Our choice for a variational ansatz is to take $u_\lambda(i) = e^{-\lambda \rho_i^2}$. This is motivated by the fact that the number of sites at a given distance from the center grows exponentially, and therefore in order to remain in the bulk of the tree, we need to cut off the wavefunction faster than exponentially.²⁸ We perform the summations by converting the sum over sites into a sum over depths, approximating the sums by integrals and using steepest-descent. We find that, at criticality, the gap is nonvanishing:

$$\Delta_{SMA}^G \sim \frac{f}{8} z \left[\frac{z - 2\sqrt{z-1}}{z - 1 + \frac{4\sqrt{z-1}}{\log(z-1)}} \right] \quad (23)$$

Excitations constrained to live in the bulk are therefore always gapped, even at criticality. The factor of $z - 2\sqrt{z-1}$ is precisely the spectral gap for bulk excitations on a Cayley tree¹. A state where $u_\lambda(i)$ is independent of position must be gapless in the broken-symmetry phase of the model, since it connects the different broken-symmetry ground states. We cannot recover this state through a correctly regulated calculation in the chosen order of limits, however.

There is a straightforward physical argument for this gap. By our choice of variational ansatz, we cut off the excitation at some depth $D \sim 1/\sqrt{\lambda}$. On a Euclidean lattice of dimension d , this costs a surface energy $\propto D^{d-1}$ which is normalized by the weight of the wavefunction $\propto D^d$. As $D \rightarrow \infty$ ($\lambda \rightarrow 0$), the SMA gap therefore vanishes as D^{-1} . On tree-like lattices, both the surface area and the bulk normalization scale as $(z-1)^D$; the boundary is always a finite fraction of the bulk. Thus, the ratio remains finite as $D \rightarrow \infty$ and the gap cannot close^{1,8}.

V. AKLT MODEL ON REGULAR RANDOM GRAPHS: FRUSTRATION AND THE SPIN GLASS STATE

We now consider the same model on a *regular random graph*⁹ of connectivity z . The ensemble of these graphs is

constructed by assigning uniform probability to all possible graphs of N vertices, such that each vertex is connected to *exactly* z links. There are several reasons why statistical models defined on this ensemble of graphs are interesting:

1. A central property of this ensemble⁹ is that typical lattices are locally tree-like; their loops have a length diverging logarithmically with the size N of the system; this implies that one can develop a method to solve statistical models on these graphs based on the same recurrence equations that are exact on trees. This is known as the *cavity method*¹⁰.
2. Despite being locally tree-like, they do not have any boundary, all sites playing statistically the same role (in the same way as periodic boundary conditions impose translation invariance on a finite cubic lattice). Moreover, the free-energy of regular random graph models is self-averaging with respect to their random character in the thermodynamic limit. In other words for large enough N a single sample is a good representative of the ensemble average.
3. Typical graphs are characterized by many large loops of even and odd length; this strongly frustrates the antiferromagnetic ordering, which gives way to a spin glass phase instead²⁹.

In the following we will be particularly interested in the implications of the last point for the quantum problem.

The reasoning outlined in section II clearly applies to the random graph model, whose AKLT ground state is therefore described by a classical Hamiltonian of the form (3), where the pairs $\langle i, j \rangle$ are connected by a link of the random graph. The main difference between the tree model and the random graph model is that the recurrence equation (5) now does not hold for the full graph; it only holds for a tree-like subregion of the graph, and has to be initialized using the boundary values of the $\psi^i(\hat{n}_i)$ that are determined by the summation over the rest of the graph. In other words, the recurrence on the subregion is initialized from random self-consistent boundary conditions, determined by the rest of the system: these boundary conditions are not consistent with Néel ordering, which is therefore frustrated, as discussed in Section III above. However, since the tree-like subregions grow in size when $N \rightarrow \infty$, equation (5) must be iterated a very large number of times. One can classify the different phases of the system by studying its fixed points^{10,11}.

To calculate the stability of the paramagnetic solution against spin glass ordering we observe that the spin glass transition is signaled, as usual, by the divergence of the classical spin glass susceptibility¹²:

$$\chi_{SG} = \frac{1}{N} \sum_{ij} [\langle \hat{n}_i \cdot \hat{n}_j \rangle]^2. \quad (24)$$

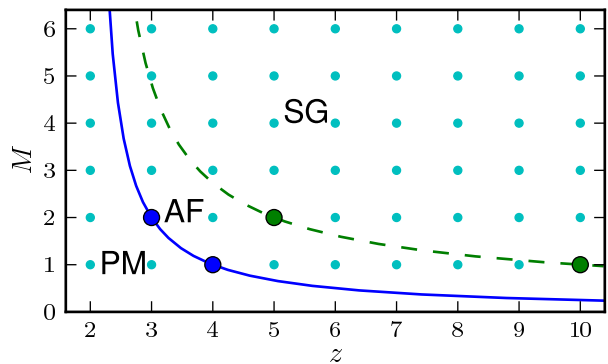


FIG. 1: Phase diagrams for AKLT model with singlet parameter M on tree-like lattices with coordination z . On the Cayley tree the transition is from paramagnetic (PM) to Néel-ordered (AF) phase at the solid blue line with no spin glass. On regular random graphs the transition is from the paramagnetic to spin glass ordered (SG) phase at the dashed green line — there is no antiferromagnet. The models with Bethe lattice critical correlations are labeled with large dots.

The details are discussed in Appendix B; the result is that χ_{SG} is finite if for all l

$$\frac{\lambda_l}{\lambda_0} \leq \frac{1}{\sqrt{z-1}}. \quad (25)$$

Once again the instability originates in the $l = 1$ sector and occurs at

$$M_{SG} = \frac{2}{\sqrt{z-1}-1} \quad (26)$$

We see that $M_{SG} = \infty$ for $z = 2$, $M_{SG} = 4.828$ for $z = 3$ (hence the system is a spin glass for $M \geq 5$), $M_{SG} = 2$ for $z = 5$ and $M_{SG} = 1$ for $z = 10$ (in these cases the system is critical), and it is smaller than 1 for any $z > 10$. See Fig. 1.

With the Néel-ordered phase suppressed, the quantum paramagnet extends further in the $z - M$ plane than on the Cayley tree models. Nonetheless, it is clear that the paramagnetic solution develops an instability to spin glass ordering at large M . What are the properties of this low temperature phase? Most of the detailed work on classical spin glasses has focussed on discrete models. The AKLT mapping provides a classical *vector* model with weakly divergent interactions whose glass phase has not yet been studied. Nonetheless, most of the qualitative features of the classical multiple-valley picture should still hold and these provide an intriguing scenario for the quantum system. The classical Gibbs measure decomposes into a collection of clustering pure states $\alpha = 1 \dots \mathcal{N}$ with essentially disjoint support. In each of these states, the $\psi_\alpha^i(\hat{n}_i)$ – and thus the local magnetizations – are macroscopically different. This strongly suggests that the quantum AKLT ground state $|\Psi\rangle$ itself is a superposition over a collection of macroscopically

distinct degenerate ground states $|\Psi_\alpha\rangle$ each of which corresponds to one of the classical clustering states.

While we believe that the above picture holds in general, a rigorous derivation is problematic. In the following we will attempt to justify it in more detail and point out some of the subtleties that must be dealt with. First, there does not yet exist a detailed study of the classical vector model³⁰ – for the purposes of this paper, we shall assume that, modulo the $O(3)$ global symmetry, the qualitative behavior is that of the better studied Ising antiferromagnet on a regular random graph¹³.

By analogy to this model, two different phases exist: at high temperatures, the stable phase is a paramagnet where $\psi^i(\hat{n}_i) = \psi(\hat{n}) = 1$ is the same for all sites, and it is the unique fixed point of Eq. (5). At low temperatures, the stable phase is a spin glass, characterized by the existence of many *non-symmetry* related pure states labeled by $\alpha = 1, \dots, \mathcal{N}$ within which connected spatial correlators vanish. This is related to the existence of many different fixed points of Eq. (5), and reflects the decomposition of the thermodynamic Gibbs measure $P = \exp(-\beta H_{cl})/Z$ as follows:

$$P(\{\hat{n}\}) = \sum_{\alpha=1}^{\mathcal{N}} w_\alpha \int dg P_\alpha(\{g \cdot \hat{n}\}) \quad (27)$$

where the P_α are representative classical pure state measures. By integrating over g , the $O(3)$ of global rotations of spin space, we account for the continuous family of symmetry related pure states associated to each representative state α . One can access these representative pure states by adding a uniform infinitesimal field to the classical model, but as the quantum AKLT state is a singlet, we prefer to work without explicitly breaking this symmetry¹².

The Ising spin glass models with two-body interactions which have been studied, such as the Sherrington-Kirkpatrick model¹⁴ and the random graph antiferromagnet¹³, are characterized by a continuous spin glass transition³¹ with a *finite* collection of pure states throughout the spin glass phase³². We shall therefore assume that this is true of our collection of representative pure states. Indeed, all we will need is that \mathcal{N} grows at most polynomially in N as the thermodynamic limit is taken.

The pure state decomposition (27) has striking consequences for the structure of the low-energy states of the quantum AKLT Hamiltonian. To wit, we argue that

$$|\Psi\rangle = \sum_{\alpha=1}^{\mathcal{N}} \sqrt{w_\alpha} \left(\int dg g \right) |\Psi_\alpha\rangle \quad (28)$$

up to exponentially small corrections in the thermodynamic limit, where the $|\Psi_\alpha\rangle$ can be interpreted as a collection of symmetry breaking degenerate quantum ground states whose correlations correspond to the classical pure states P_α .

We argue this in three parts. First, we assume the existence of a collection of quantum states $|\Psi_\alpha\rangle$ such that

$$|\langle \{\hat{n}_i\} | \Psi_\alpha \rangle|^2 = P_\alpha(\{\hat{n}_i\}) \quad (29)$$

and show that the quantum state Eq. (28) reproduces the observables of the classical decomposition of Eq. (27). Second, we will show that up to exponentially small corrections each of the $|\Psi_\alpha\rangle$ are themselves orthogonal ground states. Finally, we address the issue of the existence of such states given the classical distributions P_α .

The first part follows the argument of Ref. 15 but we rephrase it in terms of density matrices. Consider the density matrix of the proposed state Eq. (28):

$$\rho = |\Psi\rangle\langle\Psi| = \sum_{\alpha,\beta} \sqrt{w_\alpha w_\beta} \int dg' \int dg g' |\Psi_\alpha\rangle\langle\Psi_\beta| g'^{\dagger} \quad (30)$$

Given any local operator \hat{O} depending only on spins³³, its expectation value in state $|\Psi\rangle$ is given by

$$\begin{aligned} \langle\hat{O}\rangle &= \text{Tr} \rho \hat{O} \\ &= \sum_{\alpha,\beta} \sqrt{w_\alpha w_\beta} \int dg' \int dg \text{Tr} \left[g' |\Psi_\alpha\rangle\langle\Psi_\beta| g'^{\dagger} \hat{O} \right] \\ &= \sum_{\alpha,\beta} \sqrt{w_\alpha w_\beta} \int dg' \int dg \langle\Psi_\beta| g' \hat{O} g' |\Psi_\alpha\rangle \end{aligned} \quad (31)$$

We now argue that the interference term is negligible. That is,

$$\langle\Psi_\beta| g' \hat{O} g' |\Psi_\alpha\rangle = \delta_{\alpha\beta} \delta_{g'g} \langle\Psi_\alpha| g' \hat{O} g' |\Psi_\alpha\rangle \quad (32)$$

up to exponentially small corrections in the thermodynamic limit. This follows from the observation that $|\Psi_\alpha\rangle$ and $|\Psi_\beta\rangle$ have macroscopically distinct magnetization patterns that completely break the $O(3)$ symmetry. In particular, the classical configurations $\{\hat{n}_i\}$ on which the wavefunction $|\Psi_\alpha\rangle$ is concentrated have extremely small weight in any other wavefunction $\beta \neq \alpha$ – this remains true even with arbitrary global rotations allowed between them. If $\alpha = \beta$ but g and g' differ, then the configurations with weight are again macroscopically distinct by virtue of the net global rotation $g^{-1}g'$ between them. The fact that the observables are local and have bounded matrix elements does not modify these assertions. Since \mathcal{N} is finite for our antiferromagnetic model, the finite sum over the exponentially small corrections does not modify the result:

$$\langle\hat{O}\rangle = \sum_{\alpha} w_\alpha \int dg \langle\Psi_\alpha| g \hat{O} g |\Psi_\alpha\rangle \quad (33)$$

Inserting a complete set of coherent states and using Eq. (29) reproduces the classical distribution Eq. (27). The probability of finding the quantum system in a state α (with respect to the state $|\Psi\rangle$) is the same as that of the classical problem: both are given by w_α .

Furthermore, the $|\Psi_\alpha\rangle$ must have exponentially small energy with respect to the quantum Hamiltonian. Since $\langle H \rangle = 0$ in the AKLT state, using equation (33) and the rotational invariance of H , we have that

$$0 = \langle H \rangle = \sum_{\alpha} w_{\alpha} \langle \Psi_{\alpha} | H | \Psi_{\alpha} \rangle \quad (34)$$

up to exponentially small corrections. Since each of the terms in the sum is nonnegative, it follows that

$$\langle \Psi_{\alpha} | H | \Psi_{\alpha} \rangle \lesssim \mathcal{O}(e^{-N}) \quad (35)$$

Thus, the $|\Psi_{\alpha}\rangle$ are a collection of nearly orthogonal, nearly zero energy states, each of which generates a further continuous collection of such degenerate states under the action of $\mathcal{O}(3)$.

Finally, we turn to the slightly thorny question of whether states satisfying Eq. (29) exist. The problem is that the coherent state basis is overcomplete for any fixed spin size $S = zM/2$ and we cannot necessarily find quantum states which have given expansions in this basis. That is, *a priori* we cannot simply set $\langle \{\hat{n}_i\} | \Psi_{\alpha} \rangle = \sqrt{P_{\alpha}(\{\hat{n}_i\})}$ and know we have a well-defined quantum state for spins of size S . In the large spin limit, there is no problem as the coherent states become a complete, rather than overcomplete, basis. This coincides with the zero temperature limit of the classical companion model and thus the pure states $|\Psi_{\alpha}\rangle$ may be identified with the (many degenerate) minima of the energy function (3). At finite M , we cannot find such finely localized states in the coherent state representation – the most localized state has solid angular scale $\sim 1/M$ – but the finite temperature fluctuations around the classical minima will also smear the P_{α} at a similar scale.

On the other hand, we already used above that the states have disjoint support, up to exponentially small corrections in N . For a given classical configuration $\{\hat{n}_i\}$, only one state contributes to $\langle \{\hat{n}_i\} | \Psi \rangle$ significantly. Thus, in a given region of classical configuration space, $\langle \{\hat{n}_i\} | \Psi \rangle$ coincides with one of the $\langle \{\hat{n}_i\} | \Psi_{\alpha} \rangle$, and conversely, each of the $\langle \{\hat{n}_i\} | \Psi_{\alpha} \rangle$ can be seen as the restriction of the full $\langle \{\hat{n}_i\} | \Psi \rangle$ to that region. Since the $1/M$ smoothing is local in configuration space, it is safe to assume that the states $\langle \{\hat{n}_i\} | \Psi_{\alpha} \rangle$ are as smooth as the original $\langle \{\hat{n}_i\} | \Psi \rangle$, therefore $|\Psi_{\alpha}\rangle$ can be defined without ambiguity. Based on the above arguments, we think it likely that at least an approximate pure state decomposition of the form proposed above can be found even at finite M .

In summary, we obtain the following picture for the low energy spectrum in the spin glass phase: the non-clustering paramagnetic AKLT ground state $|\Psi\rangle$ can be decomposed in a superposition of several almost degenerate states, whose energies are of order $\exp(-N)$. These states enjoy the clustering property (vanishing of connected correlations) and are characterized by amorphous order (the local magnetizations are different in each state). It would be nice to check this scenario explicitly by means of exact diagonalization.

It would be very interesting to obtain more detailed information on the spectrum of such spin glass Hamiltonians. For instance, a natural question is whether there is an energy gap between the degenerate low-lying spin glass states and the excited states. Indeed, we expect Goldstone (or Halperin-Saslow) modes¹⁶ associated with twisting of the amorphously magnetized states $|\Psi_{\alpha}\rangle$. While it is difficult to explicitly construct a coarse-graining procedure to produce an effective theory of such modes on a tree-like graph, one usually expects that such a theory applies in sufficiently high dimensions¹⁷. Insofar as the effective theory is an elastic hydrodynamics living on a tree-like graph, the corresponding modes should remain gapped¹. This suggests that the low energy spectrum is indeed gapped in any given pure state sector.

VI. CONCLUDING REMARKS

In this paper, we extend the study of AKLT models to locally tree-like graphs of fixed connectivity by exploiting the quantum-classical mapping of the associated wavefunctions. On the infinite Cayley tree, we recover the results obtained in Ref. 5. We find that the Bethe lattice possesses the peculiar property that it is possible to choose parameters (for $z = 3, 4$) so that the corresponding AKLT state is *critical*. A variational calculation of the gap is unable to produce gaplessness, which is consistent with the arguments of Ref. 1 that this is a general feature of locally tree-like graphs: essentially, one cannot deform a uniform excitation into long-wavelength rotations of the order parameter, without jumping a gap in the Laplacian spectrum.

Turning to regular random graphs, we find that the companion classical model is unstable to spin glass ordering within a cavity analysis. This is a general feature of classical antiferromagnetic models on such graphs, but has striking consequences given that the peculiarities of such mean-field-like glasses should directly transfer to the *quantum* ground state of the AKLT model. This provides an alternative route to the study of quantum glassy order in tree-like models (see for example Ref. 18–23). We argue that there are now many (nearly) degenerate quantum ground states with macroscopically distinct magnetization patterns, but that there remains a gap to Halperin-Saslow waves for geometric reasons analogous to the simpler case of the antiferromagnet.

There are several avenues for future research. One obvious direction is to study the classical vector spin glass and the corresponding classical measure. In a different vein, we observe that the AKLT construction applies at a very special point in the space of quantum Hamiltonians. To what extent do the features of the quantum AKLT glass extend to regions proximate to this exactly solvable point? Ideally, the AKLT glass would capture the essential features of a broader range of quantum spin glasses, playing a role reminiscent of that played by the $S = 1$ AKLT chain in relation to the Haldane phase.

Acknowledgements

CRL and SAP thank the hospitality of the École de Physique des Houches where this work was initiated while running down locally tree-covered mountain paths. We would also like to thank Michael Aizenmann for several stimulating discussions, and for directing us to the literature on the spectral properties of random graphs. SAP and SLS would like to thank Dan Arovas for introducing them to the challenges of studying AKLT models in general dimensions and for collaboration on other work in this area. FZ wishes to thank the Princeton Center for Theoretical Science for hospitality during most of this work.

Appendix A: Transfer Matrix for the AKLT Model

The transfer matrix may be thought of as a map between functions defined on the sphere:

$$(Tf)(\hat{n}) = \int \frac{d\hat{n}'}{4\pi} T(\hat{n}, \hat{n}') f(\hat{n}') \quad (\text{A1})$$

where $\hat{n}, \hat{n}' \in S^{N-1}$. In our case, as in most cases of interest, the transfer matrix is a rotational scalar and we can work in the angular momentum basis. The eigenvalue must depend only on the L^2 eigenvalue l and not on the L_z eigenvalue m . It therefore suffices to solve the problem in the case $m = 0$.

We wish to solve the eigenvalue equation:

$$\lambda_l f_l(\hat{n}) = \int_{S^2} \frac{D\hat{n}'}{4\pi} T(\hat{n}, \hat{n}') f_l(\hat{n}') \quad (\text{A2})$$

Since the kernel T depends only on $\hat{n} \cdot \hat{n}' = \cos\theta$, we work in polar coordinates with the z -axis along \hat{n} and substitute $x = \cos\theta$ to obtain

$$\lambda_l f_l(1) = \frac{1}{2} \int_{-1}^1 dx T(x) f_l(x) \quad (\text{A3})$$

A natural guess for the eigenfunctions is that they are Legendre polynomials. The transfer matrix in our case is $T(x) = (\frac{1+x}{2})^\beta$. Using standard identities,

$$\lambda_{l,\text{AKLT}} = \frac{[\Gamma(\beta+1)]^2}{\Gamma(\beta-l+1)\Gamma(\beta+l+2)} \quad (\text{A4})$$

A similar discussion for the Heisenberg model for arbitrary N and the case of $SU(N)$ and $Sp(N)$ groups, may be found in Ref. 24.

Appendix B: Stability against spin glass ordering on a regular random graph

We follow closely the derivation of Ref. 25, Appendix A. In the thermodynamic limit, the spin glass suscepti-

bility

$$\chi_{SG} = \frac{1}{N} \sum_{ij} [\langle \hat{n}_i \cdot \hat{n}_j \rangle]^2 \quad (\text{B1})$$

can be rewritten, by taking the average over the random graphs and using translational invariance, as

$$\chi_{SG} = \sum_{d=0}^{\infty} \mathcal{N}_d [\langle \hat{n}_0 \cdot \hat{n}_d \rangle]^2 \quad (\text{B2})$$

where \mathcal{N}_d is the number of sites at distance d from a reference site. The sum is convergent as long as

$$\lim_{d \rightarrow \infty} (\mathcal{N}_d)^{1/d} [\langle \hat{n}_0 \cdot \hat{n}_d \rangle]^{2/d} \leq 1 \quad (\text{B3})$$

Note that $(\mathcal{N}_d)^{1/d} \rightarrow z - 1$ for large d . In the paramagnetic phase, $\langle \hat{n}_0 \cdot \hat{n}_d \rangle$ is given by the response of $\langle \hat{n}_0 \rangle$ (the root) to a small magnetic field coupled to \hat{n}_d , a leaf at distance d , of a tree whose other nodes are in the paramagnetic state $|00\rangle$. Hence we get (repeated indices summed):

$$\langle \hat{n}_0 \cdot \hat{n}_d \rangle \propto \frac{d\langle \hat{n}_0^i \rangle}{dh_d^i} = \int d\hat{n}_0 \hat{n}_0^i \frac{d\psi^0(\hat{n}_0)}{dh_d^i} \quad (\text{B4})$$

Clearly the term that gives the exponential dependence on d is the variation of $\psi^0(\hat{n}_0)$ with respect to h_d . Using the recursion relation (5) we can rewrite it as

$$\frac{d\psi^0(\hat{n}_0)}{dh_d} = \int d\hat{n}_1 \dots d\hat{n}_d \frac{d\psi^0(\hat{n}_0)}{d\psi^1(\hat{n}_1)} \frac{d\psi^1(\hat{n}_1)}{d\psi^2(\hat{n}_2)} \dots \frac{d\psi^d(\hat{n}_d)}{dh_d}$$

and the exponential dependence is related to the eigenvalue of the transfer matrix $\frac{d\psi^d(\hat{n}_d)}{d\psi^{d+1}(\hat{n}_{d+1})} = T(\hat{n}_d, \hat{n}_{d+1})$. These can be obtained by repeating the analysis of section III. Indeed if we use the same ket notation and write the variation $\delta|d+1\rangle = \epsilon \sum_{l \neq 0, m} c_{lm} |l m\rangle$ we can use the results of section III to obtain

$$\delta|d\rangle = \epsilon \sum_{l \neq 0, m} \frac{\lambda_l}{\lambda_0} c_{lm} |l m\rangle + \mathcal{O}(\epsilon^2) \quad (\text{B5})$$

The absence of the factor $(z-1)$ with respect to Eq. (14) is due to the fact that here we are only varying one of the neighbors of a given spin, the neighbor on the path linking the root to the given leaf at distance d . The relevant eigenvalues are therefore λ_l/λ_0 and we obtain the condition

$$(z-1) \max\{(\lambda_l/\lambda_0)^2\} \leq 1 \quad (\text{B6})$$

for the convergence of χ_{SG} .

- ¹ C. Laumann, S. Parameswaran, and S. Sondhi, Phys. Rev. B **80**, 144415 (2009).
- ² I. Affleck, T. Kennedy, E. Lieb, and H. Tasaki, Comm. Math. Phys. **115**, 477 (1988).
- ³ I. Affleck, T. Kennedy, E. H. Lieb, and H. Tasaki, Phys. Rev. Lett. **59**, 799 (1987).
- ⁴ S. Parameswaran, S. Sondhi, and D. Arovas, Physical Review B **79**, 024408 (2009).
- ⁵ M. Fannes, B. Nachtergaele, and R. Werner, J. Stat. Phys. **66**, 939 (1992).
- ⁶ D. P. Arovas, A. Auerbach, and F. D. M. Haldane, Phys. Rev. Lett. **60**, 531 (1988).
- ⁷ M. E. Fisher, Am. J. Phys. **32**, 343 (1964).
- ⁸ S. Hoory, N. Linial, and A. Wigderson, Bull. Amer. Math. Soc. **43**, 439 (2006).
- ⁹ S. Janson, T. Luczak, and A. Ruciński, *Random graphs* (Wiley-Interscience Series in Discrete Mathematics and Optimization, 2000).
- ¹⁰ M. Mezard and G. Parisi, The European Physical Journal B-Condensed Matter and Complex Systems **20**, 217 (2001).
- ¹¹ M. Mézard and A. Montanari, *Information, physics, and computation* (Oxford University Press, USA, 2009).
- ¹² K. Binder and A. Young, Rev. Mod. Phys. **58**, 801 (1986).
- ¹³ F. Krzakala and L. Zdeborová, EPL (Europhysics Letters) **81**, 57005 (2008).
- ¹⁴ M. Mézard, G. Parisi, and M. Virasoro, *Spin glass theory and beyond* (World Scientific, Singapore, 1987).
- ¹⁵ G. Biroli, C. Chamon, and F. Zamponi, Physical Review B **78**, 224306 (2008).
- ¹⁶ B. I. Halperin and W. M. Saslow, Phys. Rev. B **16**, 2154 (1977).
- ¹⁷ V. Gurarie and J. Chalker, Phys Rev B **68**, 134207 (2003).
- ¹⁸ C. R. Laumann, A. Scardicchio, and S. L. Sondhi, Phys. Rev. B **78**, 134424 (2008).
- ¹⁹ T. K. Kopec and K. D. Usadel, Phys. Stat. Sol. (b) **243**, 502 (2006).
- ²⁰ T. K. Kopec and K. D. Usadel, Phys. Rev. Lett. **78**, 1988 (1997).
- ²¹ M. Tarzia and G. Biroli, Europhys. Lett. **82**, 67008 (2008).
- ²² G. Carleo, M. Tarzia, and F. Zamponi, Phys. Rev. Lett. **103**, 215302 (2009).
- ²³ T. Jorg, F. Krzakala, G. Semerjian, and F. Zamponi (2009), arXiv:0911.3438.
- ²⁴ P. Fendley and O. Tchernyshyov, Nucl. Phys. B **639**, 411 (2002).
- ²⁵ L. Zdeborová and F. Krzakala, Phys. Rev. E **76**, 031131 (2007).
- ²⁶ A. C. C. Coolen, N. S. Skantzos, I. P. Castillo, C. J. P. Vicente, J. P. L. Hatchett, B. Wemmenhove, and T. Nikoletopoulos, Journal of Physics A: Mathematical and General **38**, 8289 (2005).
- ²⁷ A few comments on the nature of the classical statistical state space of a vector spin are in order, as we have so cavalierly complexified and tensored it into a much more quantum mechanical looking system. Physical cavity distributions $\psi(\hat{n})$ must be real, normalizable, nonnegative functions on the sphere. By its construction as a marginalization (summing out) procedure, equation (10) must produce such a physical output given physical inputs, even though we have extended it over \mathbb{C} . A more important subtlety arises in the normalization of states – the standard L^2 norm associated with the Dirac inner product is not necessarily 1 for a properly normalized probability distribution. Since the probabilistic L^1 norm is incompatible with the Hilbert space structure, it is much simpler to work with unnormalized vectors and keep in mind that a probabilistic interpretation only applies in the standard basis.
- ²⁸ In principle, an exponential regulator with a sufficiently fast decay constant also works. The calculation proceeds in a similar fashion but the interpretation is more complicated and no more enlightening.
- ²⁹ See Ref. 10 for a general discussion and Ref. 13 for the explicit computation of the phase diagram of a classical Ising antiferromagnet.
- ³⁰ Although there is a replica symmetric treatment of a related model with the additional complication of random interactions. See Ref. 26.
- ³¹ Other mean field spin glass models, such as the p -spin model, can have a number of states scaling exponentially in system size. These models show a discontinuous spin glass transition. However, antiferromagnetic models with two-body interactions usually do not show this phenomenology, therefore we will not investigate this transition in this paper.
- ³² See Ref. 14, and in particular the reprint on page 226, for a more detailed discussion of this delicate statement.
- ³³ Such observables are diagonal in the coherent state basis and therefore their correlations follow from the classical measure.